

Surface Energy Calculation for a *fcc* Metal Gold (Au) Using the GEAM

A. A. Oni-Ojo, S. Onwusinkwue, E. O. Aiyohuyin and J. O. A. Idiodi

Department of Physics, University of Benin, Benin City, Nigeria.

Abstract

*The surface energy of *fcc* metal Au is here calculated for the three low-index surface using the generalized embedded-atom method (GEAM). The (III) surface was found to have the lowest energy while the (110) surface had the highest energy, with the energy of the (100) surface in between. The predicted results are in good agreement with the experimental values.*

1.0 Introduction

Surface energy is an important quality for understanding many surface phenomenon such as absorption, corrosion, crystal growth etc.

Surface energy for metals with face-entered cubic (*fcc*), body-cantered cubic(*bcc*) and diamond structure [1-7] have been calculated by the embedded – atom method (EAM) developed by Daw and Baskes [7,8]. However, the EAM prediction, for single crystal surface energy is about 50% below polycrystalline experimental value [2].

There has been the need to improve on the original work of Daws and Baskes which led to several modifications such as the modified embedded-atom method (MEAM)[2,3,9], the analytical embedded atom method (AEAM) by Johnson et al [10-13] and the modified analytical embedded atom method (MAEAM) by Zhang et al[14]

In this paper, the surface energy of *fcc* metal Au is here calculated using the generalized embedded atom method (GEAM).

The other parts of this paper are organised as follows: Section 2 of the paper deals with Basic **EAM** equations. The **EAM** parameters and methods of calculating them are discussed in section 3, the surface energy and cohesive energy curves are presented in 4, while conclusion is given in section 5.

2.0 Basic EAM Equations for *fcc* Metals

In the EAM, the total energy of a system E_t is approximated by

$$E_t = \sum_{j=1}^N F_i(\rho_{i,j}) + \frac{1}{2} \sum_{i,j} \Phi_{i,j}(R_{i,j}) \quad (2.1)$$

Where $F(\rho)$ is the energy to embed an atom into the background electron density $\rho(R)$ at site i, $\Phi_{i,j}(R)$ is the screened pair potential between atoms i and j.

It is good to note here, that in practice, functional forms are chosen for $F_i(\rho_{i,j})$ and $\Phi_{i,j}$ and that the parameters in these functions are determined by fitting to a limited number of bulk properties. If U_0 denotes the total energy per atom (negative of the cohesive energy E_0) and $\rho_{i,j}$ in the electron density function at position R, then within a nearest neighbour model, it can be shown that, for a monoatomic *fcc* solid [7,15-18]

$$U_0 = 6\phi_1(r_0) + F(\rho_0) \quad (2.2)$$

$$0 = \phi_1(r_0) + 3F(\rho_0) V_1 / r_0 \quad (2.3)$$

$$\frac{3aB_0}{4} = \phi_1(r_0) + \frac{a}{4} \left\{ F(\rho_0) [2W_1 - 8W_1 - 5V_1] \right\} - \frac{a}{4} \left\{ 2F(\rho_0)V_1^2 \right\} \quad (2.4)$$

$$\frac{a}{4} C_1 = G_1 + \frac{a}{4} F(\rho_0) W_1 + \frac{a}{4} F(\rho_0) V_1^2 \quad (2.5)$$

$$\frac{a}{4} C_2 = G_1 + \frac{a}{4} F(\rho_0) W_1 + \frac{a}{4} F(\rho_0) V_1^2 \quad (2.6)$$

$$\frac{a}{4} C_4 = G_1 + \frac{a}{4} F(\rho_0) W_1 \quad (2.7)$$

Corresponding author: A. A. Oni-Ojo, E-mail: amenaghawon.oni-ojo@uniben.edu, Tel.: +2348056284393

$$\text{where } G_1 = \frac{\phi_1(r_0)}{2r_0} + \frac{\phi_1(r_0)}{2} \quad \dots \quad (2.8)$$

$$\text{and } G_1 = \frac{-E\phi_1(r_0)}{q(r_0)} + \frac{\phi_1(r_0)}{q} \quad \dots \quad (2.9)$$

The equations(2.2) – (2.7), constitute the basic equations of the EAM and they depend on the fundamental functions $F(\rho)$, $\rho(\mathbf{r})$ and $\phi(\mathbf{r})$.

The monovacancy formation energy E_{ti}^f is of the form

$$E_{\text{ti}}^f = 12F\left(\frac{11}{12}\rho_0\right) - 11F(\rho_0) - U_0 \quad \dots \quad (2.10)$$

In this work, E_{ti}^f is considered as a known physical input.

From (2.7) and (2.6), we get

$$V_1 = \pm \sqrt{\frac{\Omega_0(C_1 - C_4)}{F(\rho_0)}} \quad \dots \quad (2.11)$$

For metals with $C_1 > C_4$, we demand that $F(\rho_0)$ be positive definite while for metal with $C_1 < C_4$, $F(\rho_0)$ must be negative definite[18].

3.0 GEAM Parameter/Calculation Method

In an earlier study, Oni-Ojo et al [18] proposed a generalized embedded function $F(\rho)$ by modifying the work of Yuan *et al* [19]to a robust and flexible embedding function.

$$F(\rho) = AE_0\left(\frac{\rho}{\rho_0}\right)^A \left[\ln\left(\frac{\rho}{\rho_0}\right)^a - k \right] \quad \dots \quad (3.1)$$

Where A and K consist in providing the flexibility. From 3.1, we obtain the three EAM parameters

$$F(\rho_0) = -AE_0k \quad \dots \quad (3.2)$$

$$F'(\rho_0) = \frac{-F(\rho_0)}{\rho_0} \left[\lambda - \frac{a}{K} \right] \quad \dots \quad (3.3)$$

$$F''(\rho_0) = \frac{F(\rho_0)}{\rho_0^2} \left[\lambda^2 - \frac{2a}{K} + \frac{a}{K} - \lambda \right] \quad \dots \quad (3.4)$$

The prime in (3.3) and (3.4) denotes differentiation with respect to the electron density, q. In this studies, we have obtained results for $A = +1$ and $A = -1$, and the parameter A and K are chosen by demanding that the embedding function $F(\rho)$ satisfy equation (2.10) and hence,

$$\lambda = \frac{\frac{1}{2}\left[\frac{1}{2}E_{\text{ti}}^f + \frac{1}{2}F(\rho_0) + U_0\right]}{\frac{1}{2}\left(AE_0\left|\frac{1}{2}\left(\frac{1}{2}E_{\text{ti}}^f + U_0\right)\right| - K\right)} \quad \dots \quad (3.5)$$

With, λ and K known, the EAM functions and the EAM parameters are determined thereafter. The result as shown in Table 2 using the input parameters in Table 1.

Table 1: Table of input Parameters for Au

Lattice Constant a (\AA), Bulk Modulus (GPa) Elastic Constant (GPa), Cohesive and monovacancy formation energy (eV)

	Cohesion energy E_0 (eV)	Monovacancy Formation energy (eV)	Lattice Constant a (A)	Elastic constant (Gpa)			Bulk Modulus B (GPa)
				C_{11}	C_{12}	C_{44}	
Au	3.93	0.89	4.08	1.89	1.59	0.42	1.73

Table 2: EAM Parameters

Parameter	Model					
	I	II	III	IV	V	VI
A	-1	1	-1	-1	1	1
α	0.06	0.06	0.1	0.62	1.05	1.9
K	0.2	-0.2	0.2	0.2	0.05	0.9
λ	6.275493	5.675356	6.46877	8.723907	2.852125	2.073475
$F(\rho_0)$ [eV]	0.786	0.786	0.786	0.786	-0.1965	-3.537
$F(\rho_0)[\text{eV}/\rho_0]$	4.696737	4.69663	4.691453	4.420391	3.566057	0.13312
$F(\rho_0)[\text{eV}/\rho_0^2]$	23.29784	23.29667	23.11425	12.88601	18.37408	15.62554
$V_{11}[\rho_0]$	-0.72952	-0.72954	-0.73241	-0.98093	-0.82147	-0.8908
$W_{11}[\rho_0]$	-5.16513	-5.16525	-5.17509	-5.89963	-6.52411	-132.54
$W_{12}[\rho_0]$	-1.35	-1.35	-1.35	-1.33	-1.85	-6.02E+01
$\phi_1(r_0)$ [eV]	-0.786	-0.786	-0.786	-0.786	-0.62225	-0.0655
$\phi_1(r_0)[\text{eV}/\text{\AA}]$	0.593826	0.593828	0.595509	0.751489	0.507699	0.020552
$\phi_1(r_0)[\text{eV}/\text{\AA}^2]$	3.63	3.63	3.63	3.79	3.54	3.03

4.0 Surface Energy and Cohesive Energy Curves

The total energy for three low-index surface for gold (Au) is calculated for the various GEAM values for **A**, **λ** , **α** and **K** [20] and are presented in Table 3

Table 3: Table of thee predicted low-index surface energy for Au in Ergs/cm² and the average experimental value for Au is taken from ref.[15]

Model	Present work				EXPERIMENT
	111	100	110	AVERAGE	
I	1185.589	1646.267	1747.97	1526.61	1500.00
II	1185.47	1646.113	1747.85	1526.48	
III	1184.35	1645.131	1747.32	1525.60	
IV	1142.23	1612.374	1731.69	1495.43	
V	1157.60	1641.61	1777.59	1525.60	
VI	1120.84	1609.34	1771.89	1500.70	

With the surface energy obtained, this work shall be extended by studying the total energy curve.

In the GEAM, simple density function $\rho(r)$ as can be found in other EAM is chosen;

$$\dots(r) = \dots_o e^{-s\left(\frac{r}{r_0}-1\right)} \quad (4.1)$$

But for the pair potential function, we have

$$W_1(r) = B_1 e^{-p\left(\frac{r}{r_0}-1\right)} + B_2 e^{-p\left(\frac{2}{\sqrt{3}}\frac{r}{r_0}-1\right)} \quad (4.2)$$

With the value of s , B_1 , B_2 and P determined, (see Table 4), the cohesive energy is calculated, ie,

$$U(r) = 6\phi_1(r) + F(r) \quad (4.3)$$

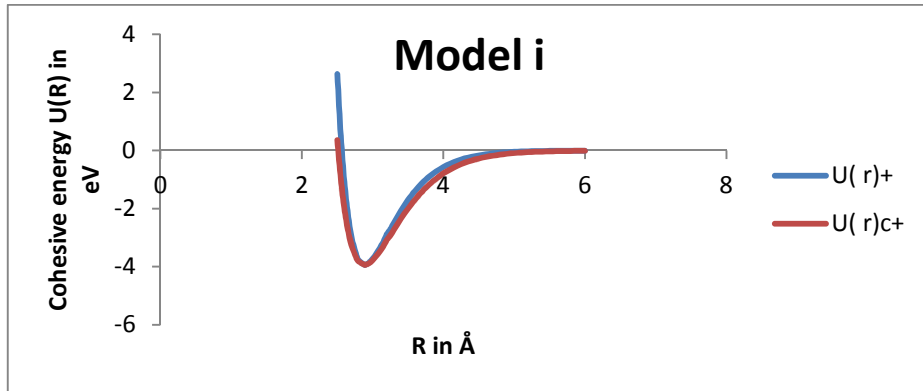
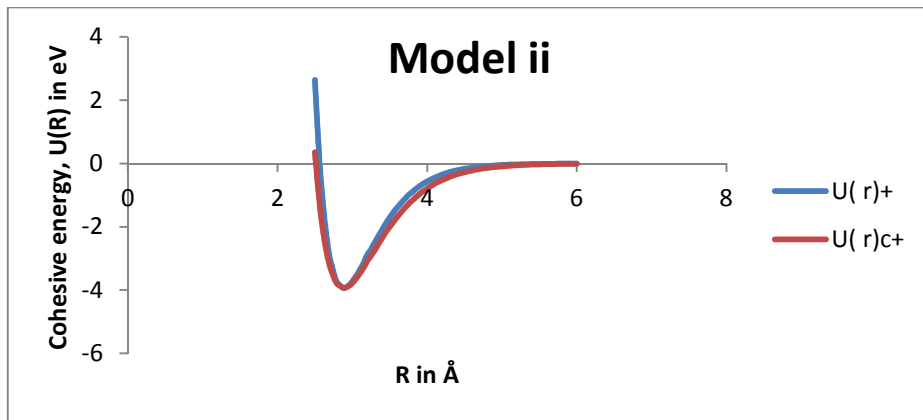
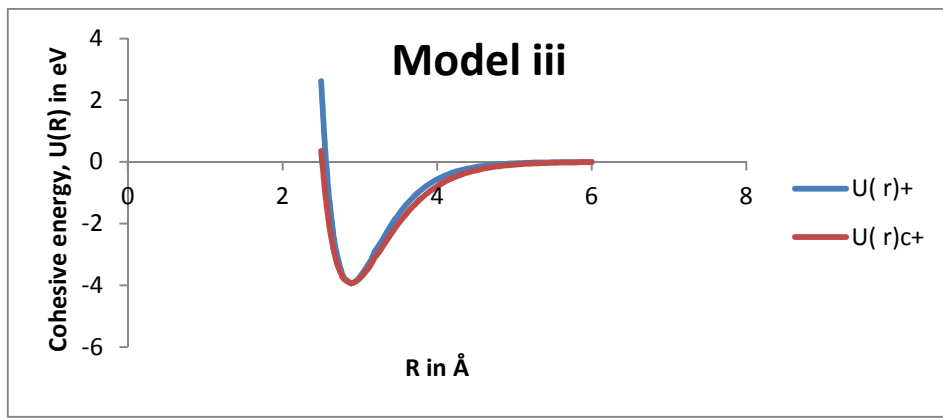
And is compared with the cohesive energy function of Rose *et al* [21]

$$U(r) = U_0 \left[1 + r_R \left(\frac{r}{r_0} - 1 \right) \right] e^{-r_R \left(\frac{r}{r_0} - 1 \right)} \quad (4.4)$$

$$\text{Where: } r_R^2 = \frac{9\Omega_0 B}{E_c} \quad (4.5)$$

Table 4: Parameters for cohesive energy curve

Parameter	Models					
	I	II	III	IV	V	VI
	2.19	2.19	2.20	2.94	2.46	2.67
p	8.15	8.15	8.16	9.01	8.97	19.12
B ₁	-4.51	-4.51	-4.51	-4.31	-3.59	-0.47
B ₂	13.13	13.14	13.14	14.20	11.87	7.77

**Fig. 1:** Graph of the cohesive energy curve of GEAM prediction for Au with values of A=-1, $\alpha=0.06$, K=0.2 and $\lambda=6.275493$ and that of Rose et al[21]**Fig. 2:** Graph of the cohesive energy curve of GEAM prediction for Au with values of A=1, $\alpha=0.06$, K=-0.2 and $\lambda=5.675356$ and that of Rose et al[21]**Fig. 3:** Graph of the cohesive energy curve of GEAM prediction for Au with values of A=-1, $\alpha=0.1$, K=0.2 and $\lambda=6.46877$ and that of Rose et al[21]

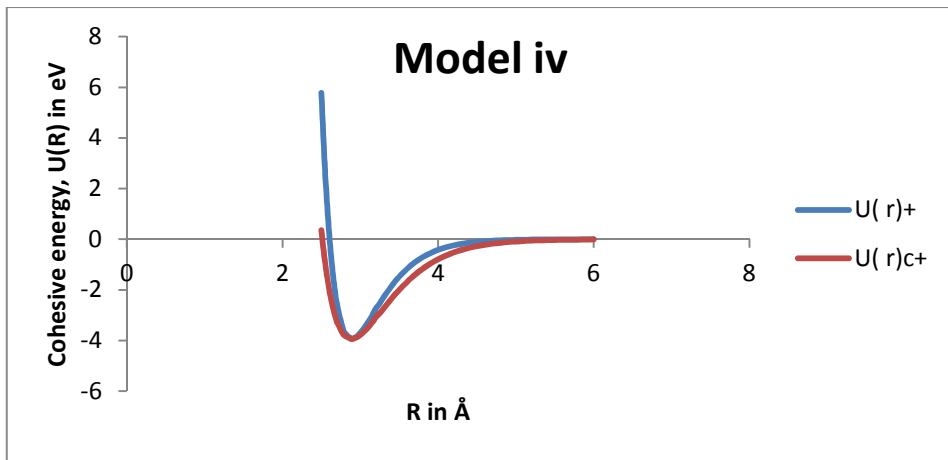


Fig. 4: Graph of the cohesive energy curve of GEAM prediction for Au with values of $A=1$, $\alpha=0.62$, $K=0.2$ and $\lambda=8.723907$ and that of Rose et al[21]

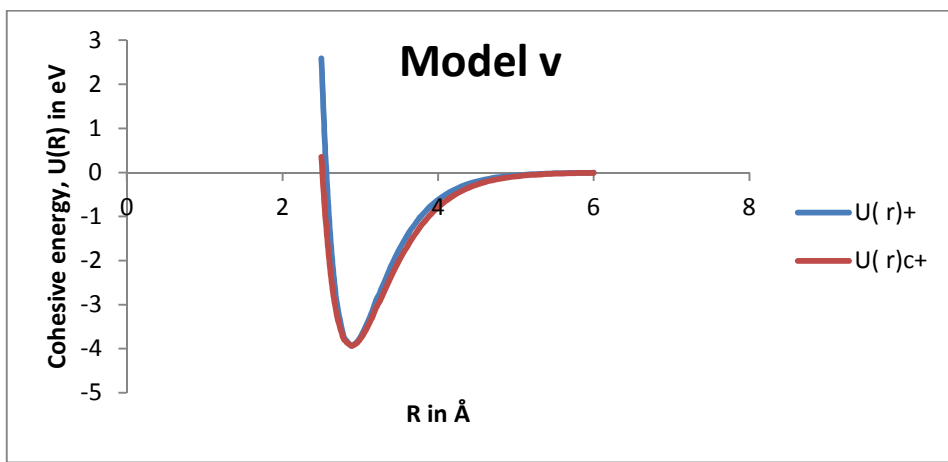


Fig. 5: Graph of the cohesive energy curve of GEAM prediction for Au with values of $A=1$, $\alpha=1.05$, $K=0.05$ and $\lambda=2.852125$ and that of Rose et al[21]

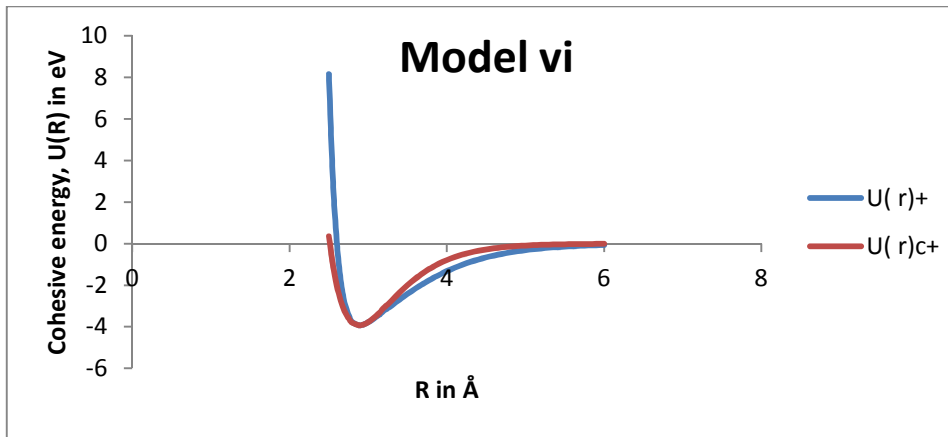


Fig. 6: Graph of the cohesive energy curve of GEAM prediction for Au with values of $A=1$, $\alpha=1.9$, $K=0.9$ and $\lambda=2.073475$ and that of Rose et al[21]

5.0 Conclusion

The three low-index surface energy of Au has been calculated using the GEAM, and the results obtained reveal $\langle 111 \rangle < \langle 100 \rangle < \langle 110 \rangle$ for all the values and their average is in good agreement with experimental average. The curve of the cohesive energy obtained with the GEAM, also show good agreement with the cohesive energy curve of the Rose et al. Thus, the GEAM will be a good tool for estimating relative values of surface energy and other properties of metals.

6.0 References

- [1] J.B Adams, S.M Foiles, Physical Review B41 (1999), 3316.
- [2] M. I Baskes, Physical Review B46 (1992), 2727.
- [3] M.I Baskes, J. S Nelson, A. F Wright, Physical Review B40 (1989), 6085.
- [4] J. R Smith, ABenerjea, Physical ReviewLett. 59 (1987), 2451.
- [5] S. M Foiles, M, I Baskes, M. S Daw, Physical Review B33 (1986), 7983.
- [6] R. A Johnson, Physical Review B37 (1988), 3924.
- [7] M. S Daw, M. I Baskes, Physical Review B29 (1984), 1285.
- [8] M. S Daw, M. I Baskes, Physical ReviewLett. 50 (1983), 1285.
- [9] M. I Baskes, Physical ReviewLett. 59 (1987), 2666.
- [10] R. A Johnson, Physical Review B37 (1988), 3924.
- [11] R. A Johnson, D. J Oh, J. Mater Res. 4 (1989), 1195.
- [12] D. J Oh, R. A Johnson, J. Mater Res. 3 (1988), 471.
- [13] R. A Johnson, Physical Review B41 (1990), 471.
- [14] Yan-Wi Wen, Jian-Min Zhang, Computational material science 42(2008), 281.
- [15] Aghemenloh E and Idiodi J. O. A. ,J.Nig. Math. Phys. Vol.2. (1998), 271.
- [16] J. O. Alidodi and E. Aghemenloh, J. Nig Ass. Math. Phys. Vol 2.(1998), 285.
- [17] J. O. Alidodi and E. Aghemenloh, J. Nig Ass. Math. Phys. Vol 3.(1999), 167.
- [18] Oni-Ojo A. A, Idiodi J. O. A and Aiyohuyin E. O, J. Nig Ass. Math. Phys. Vol 11 (2007), 509.
- [19] X. Yuan, K. Takahashi, Y. Yin and T. Onzawa, modelling simul. Mater. Science. Eng. Vol. 11.(2003),447.
- [20] Oni-Ojo A. A, M.PhilThesis,University of Benin (2010)
- [21] Rose J. H, Smith J. R, Guinea F and Ferrante J, Phys. Rev. B 29 (1984), 2963